Export of calcium carbonate corrosive waters from the East Siberian Sea

Leif G. Anderson[1], Jörgen Ek[2], Ylva Ericson[3], Christoph Humborg[2,4], Igor Semiletov[5,6,7], Marcus Sundbom[2], Adam Ulfsbo[1,8]

[1]Department of Marine Sciences, University of Gothenburg, 412 96 Gothenburg, Sweden
5 [2]Baltic Sea Centre, Stockholm University, 106 91 Stockholm, Sweden
[3]The University Centre in Svalbard, Pb 156, 9171 Longyearbyen, Norway
[4]Department of Environmental Science and Analytical Chemistry, Stockholm University, 106 91 Stockholm, Sweden
[5]International Arctic Research Center, University Alaska Fairbanks, Fairbanks, AK 99775, USA
[6]Pacific Oceanological Institute, Russian Academy of Sciences Far Eastern Branch, Vladivostok 690041, Russia
10 [7]The National Research Tomsk Polytechnic University, Tomsk, Russia
[8]Division of Earth and Ocean Sciences, Nicholas School of the Environment, Duke University, Durham, NC 27704, USA

Correspondence to: Leif G. Anderson (leif.anderson@marine.gu.se)

Abstract. The Siberian Shelf Seas are areas of extensive biogeochemical transformation of organic matter, both of marine and terrestrial origin. This in combination with brine production from sea ice formation results in a cold bottom water of
15 relative high salinity and partial pressure of carbon dioxide (pCO_2). Data from the SWERUS-C3 expedition compiled on the icebreaker Oden in July to September 2014 show the distribution of such waters at the outer shelf, as well as their export into the deep central Arctic basins. Very high pCO_2 water, up to close to 1000 µatm, was observed associated with high nutrients and low oxygen concentrations. Consequently the saturation state of calcium carbonate was low, down to less than 0.8 for calcite and 0.5 for aragonite. Waters undersaturated in aragonite were also observed in the surface in waters at equilibrium
20 with atmospheric CO_2, however, at these conditions the cause of under-saturation was low salinity from river runoff and/or sea ice melt. The calcium carbonate corrosive water was observed all along the continental margin and well out into the deep Makarov and Canada Basins at a depth from about 50 m depth in the west to about 150 m in the east. These waters of low aragonite saturation state are traced in historic data to the Canada Basin and in the waters flowing out of the Arctic Ocean north of Greenland and in the western Fram Strait, thus potentially impacting the marine life in the North Atlantic
25 Ocean.

1 Introduction

Biogeochemical processes in the Arctic Ocean can have a much greater impact on Ocean Acidification than that of anthropogenic CO_2. Investigation of the East Siberian shelf area illustrates the substantial impact of organic matter decay on lowering pH and thus also the calcium carbonate solubility state (Semiletov et al., 2016). The high corrosive shelf water
30 spreads far out into the deep central Arctic Ocean and potentially further into the North Atlantic Ocean (Azetsu-Scott et al., 2010). Here it can have negative effects on aragonite-shelled pelagic organisms like the pteropods, which are important in the Arctic Ocean and North Atlantic food web.

The decrease of pH in the ocean as a result of uptake of anthropogenic carbon dioxide (CO_2) from the atmosphere is noted Ocean Acidification (e.g. Doney et al., 2009). The change in pH caused by the increase of partial pressure of CO_2 (pCO_2) from about 280 µatm in preindustrial times to about 400 µatm today is in the order of 0.1 pH unit. A continued usage of fossil fuels at the present rate has been projected to lead to an atmospheric level of close to 1000 µatm at the end of this

5   decade, resulting in a further decrease of pH by about 0.3 units in oceanic surface waters (e.g. Orr et al., 2005). Changes in pH of this range will likely impact the marine ecosystem as well as society (e.g. Gattuso et al., 2015).

The Arctic Ocean is one of the oceans that experience the lowest natural pH, a result of the high gas solubility in cold waters. On the other side the change in pH for a given increase in pCO_2 is less in cold waters than in warm, as the buffer capacity for CO_2 is less. However, there are several other processes than air-sea exchange of CO_2 that impacts pH of Arctic waters.

10   Some Arctic shelf seas are among the most productive of the world oceans and as such experience large natural seasonal variability in pCO_2 and pH. One consequence of the high primary productivity in the inflow shelf seas (Carmack and Wassmann, 2006) is that the surface waters of the central Arctic Ocean largely are undersaturated in CO_2 (Jutterström and Anderson, 2010). This is a result of the waters being covered by sea ice that hampers air-sea flux, before the atmospheric exchange compensates for the CO_2 taken up by the phytoplankton. Decreased summer sea ice cover in the central Arctic

15   Ocean will likely reduce this effect and adjust the surface water closer to atmospheric equilibrium.

Increased pCO_2 levels decrease carbonate ion (CO_3^{2-}) concentrations, which also reduces the solubility of calcium carbonate crystals, illustrated by the reaction;

$$CaCO_3(s) \leftrightarrows Ca^{2+} + CO_3^{2-} \qquad (1)$$

Where the solubility is determined by the chemical solubility product, K_{so}, which is the product of the calcium and carbonate

20   ion concentrations, i.e. $K_{so} = [Ca^{2+}] \times [CO_3^{2-}]$. In the ocean K_{so} is dependent on temperature, salinity and pressure. To determine if the conditions are such that calcium carbonate is supersaturated or undersaturated one often uses the solubility state, Ω.

$$\Omega = \frac{[Ca^{2+}] \times [CO_3^{2-}]}{K_{so}} \qquad (2)$$

Hence, if Ω is less than 1 the water is undersaturated and if greater than 1 it is supersaturated.

25   Calcium carbonate crystals can have different structures, each with a specific K_{so}. The most common are calcite and aragonite, but in cold environments like sea ice also ikaite can form (e.g. Dieckmann et al., 2008). Calcite and aragonite are mainly formed by biological calcification where calcium carbonate is produced as part of an organism's structure. Even if the crystals are built up of carbonate ions it is in most cases hydrogen carbonate ions (HCO_3^-) that are extracted by the organisms from seawater and converted to CO_3^{2-} internally (e.g. Findlay et al., 2011). Thus there might not be a direct

30   coupling between the biological formation rate of $CaCO_3$ minerals and ocean acidification. However, the opposite reaction, i.e. dissolution of $CaCO_3$ minerals, is influenced by ocean acidification through the solubility state, at least as long as the crystals are directly exposed to seawater.

Among the biologically produced calcium carbonates, aragonite is more soluble than calcite making the former more sensitive to ocean acidification. During biological formation of calcite, magnesium can be incorporated instead of calcium, which increases the solubility; the higher the content of magnesium, the higher the solubility. High-magnesium calcite has a higher solubility than aragonite making this the most sensitive form. A range of these mineral forms are produced by

5   organisms living in the Arctic Ocean. Among those producing aragonite skeletons are cold-water corals and pteropodes, while most benthic organisms tend to produce a larger fraction of calcite. Consequently there is a substantial diversity in the biological produced $CaCO_3$ minerals and thus also different sensitivities to ocean acidification.

In this contribution we show the importance of the Siberian shelves in producing calcium carbonate undersaturated waters that spread out into the deep Arctic Ocean and further towards the Atlantic Ocean. The processes behind the under-

10   saturation are elucidated as well as the flow path of this signature in the Arctic Ocean.

2 Methods

This contribution is based on data that were collected during the SWERUS-C3 (Swedish – Russian – US Arctic Ocean Investigation of Climate-Cryosphere-Carbon Interactions) expedition with the Swedish icebreaker *Oden* along the outer Siberian shelf and covers a longitudinal range between about 125 ^{o}E to 175 ^{o}W (see Figure 1 for station positions).

15   Sampling was intensified across the shelf break along sections (A-F). Furthermore, historic data are used to evaluate how the waters from the Siberian shelf are spread out in the central Arctic Ocean and further towards Fram Strait on their way to the North Atlantic Ocean. These include data from north of Greenland collected during the Oden 1991 cruise (Anderson et al., 1994), data from the northern Fram strait collected in 2002 (Jutterström et al., 2008), and data from the Canada Basin collected in 2005 (Jones et al., 2008a).

20   The SWERUS-C3 data were gathered at about 100 stations, occupied between 15 July and 25 September 2014. Water samples were collected using a rosette system equipped with 24 bottles of Niskin type, each having a volume of 7 L. The bottles were closed during the return of the CTD-rosette package from the bottom to the surface and water samples for all constituents were drawn soon after the rosette was secured in the CTD container.

The following constituents are used; dissolved inorganic carbon (DIC) (only stations visited after 24 August), total alkalinity

25   (TA), pH, oxygen, nutrients, and bottle salinity. The order of sampling was determined by the risk of contamination meaning that oxygen samples were collected first followed by the carbonate system parameters, the nutrients, and salinity. Water samples for salinity were analysed for more than 90% of the depths and when no data were available the CTD salinity was used. Temperature data were taken from the CTD.

Salinity and temperature data were collected using a SeaBird 911+ CTD with dual SeaBird temperature (SBE 3),

30   conductivity (SBE 04C) and oxygen sensors (SBE 43) attached to the rosette system. Salinity was calibrated against deep water samples analysed on board using an AUTOSAL 8400B lab-salinometer. The salinometer was calibrated using one standard sea water ampoule (IAPSO standard sea water, OSIL Environmental Instruments and Systems) before each batch of

24 samples. The accuracy of the Autosal salinities and CTD salinities were both within ±0.003 psu and the accuracy for temperature ±0.002 ^{o}C.

DIC was determined by a coulometric titration method based on Johnson et al. (1987), having a precision of 2 µmol kg^{-1}, estimated from duplicates, with the accuracy set by calibration against certified reference materials (CRM), supplied by A.

5   Dickson, Scripps Institution of Oceanography (USA). TA was determined by automated open-cell potentiometric titration (Haraldsson et al., 1997), precision better than 2 µmol kg^{-1}, with the accuracy set the same way as for DIC. Seawater pH was determined by a spectrophotometric method, based on the absorption ratio of the sulphonephtalein dye, *m*-Cresol Purple (mCP) (Clayton and Byrne, 1993). Purified mCP (Liu et al., 2011) was purchased from the laboratory of Robert H. Byrne, University of South Florida, USA. The accuracy was estimated to 0.006 from internal consistency calculations of analyzed

10   CRM samples and the precision, defined as the absolute mean difference of duplicate samples, was ~0.001 pH units.

Oxygen was measured by an automated Winkler titration system giving a precision of ~1 µmol kg^{-1}. The accuracy was set by titrating known amounts of KIO_3 salts that were dissolved in sulphuric acid. As the amount was known to better than 0.1% the accuracy should be significantly better than the precision. The deviation from saturation concentration was computed as apparent oxygen utilization (AOU) as $[O_2]^{sat} - [O_2]^{measured}$.

15   Dissolved inorganic nitrogen species (NH_4, NO_2+NO_3), orthophosphate (PO_4) and dissolved silicate were measured on board using a four-channel continuous flow analyser (QuAAtro system, SEAL Analytical). Within each analysis run a calibration was done using standard solutions of NH_4Cl, KNO_3, K_2HPO_4 and a commercial stable silica-compound solution. Analysis quality was further assured by automatic drift control using standard solutions and always including CRM solutions prepared from commercial ampoules (QC RW1, Batch VKI-9-3-0702) in the analysis run. Accuracy expressed as the median

20   deviation of the measurements from the CRM solution for NH_4, NO_2+NO_3 and PO_4 was -0.15, -0.11, and -0.018 µmol L^{-1}, respectively. The CRM is not certified for silicate. The precision was, based on 28 determinations of standards, 3.7%, 1.2%, 2.7% and 1.3% for NH_4, NO_2+NO_3, PO_4 and SiO_4, respectively.

The saturation states of the two major forms of calcium carbonate ($\Omega^{aragonite}$ and $\Omega^{calcite}$) and pCO_2 were calculated from the combination of pH and TA, as well as pH and DIC when the latter was available, using CO2SYS (van Heuven et al., 2011)

25   with the carbonate dissociation constants (K_1 and K_2) of Lueker et al. (2000). When two computations were performed the reported values are the average of the two calculated for each sample. Input data included salinity, temperature, PO_4 and SiO_4 data. The uncertainty was computed using a Monte Carlo approach (Legge et al., 2015) and expressed as double standard deviation was about 2.5% for pCO_2 and less than 1% for Ω.

3 Results

30   The very large shelf areas north of Siberia are heavily impacted by river input, adding fresh water and chemical constituents. The direct addition of high pCO_2 runoff together with biochemical processes such as primary production and decay of organic matter, of both marine and terrestrial origin, strongly impact the calcium carbonate saturation state. The distribution

of this specific water characteristic on the shelf as well as its export into, and circulation within, the deep basins is determined by the atmospheric pressure field that drives the oceanic currents.

Low calcium carbonate saturated water was observed along the bottom of the shelf at most stations (Figure 2), associated with high nutrient and low oxygen concentrations. The strongest signal was north of the New Siberian Islands, a local

5 minimum in saturation state at about 157 ^{o}E followed by a less strong signal further to the east. Low saturation state with under-saturation in aragonite was also observed in the surface water north of the New Siberian Islands. This water had low salinity, high phosphate, as well as high silicate concentrations and relatively high pCO_2 despite having nitrate concentrations as low as about 0.2 µmol/L.

The extension of this high pCO_2 and low $\Omega^{aragonite}$ water out into the deep basin was seen in a layer centred at about 100 m

10 depth all along the shelf break from the east of the Lomonosov Ridge to 180 ^{o}E (Figure 3). Over the Lomonosov Ridge (section A) there was a faint minimum in $\Omega^{aragonite}$ even if the waters never were undersaturated. Moving east to section B undersaturated waters were observed both in the surface and at approximately 50 m depth. Further to the east, sections C, D and E, have strong $\Omega^{aragonite}$ minima centred at ~100 m depth. In the most eastern section of this study, section F, the minimum was less intense and was also found at somewhat greater depth, ~150 m. In all sections the minimum in $\Omega^{aragonite}$

15 was closely followed by a maximum in pCO_2 (Figure 3). In section C and even more so in D and E the $\Omega^{aragonite}$ minima were observed in close vicinity to the sediment.

This low saturated water has been observed in the Canada Basin on several occasions (e.g. Yamamoto-Kawai et al., 2009; Anderson et al., 2010). During the Beringia 2005 expedition where $\Omega^{aragonite}$ levels as low as 0.6 were observed at 100 m depth (Figure 4), the layer of under-saturation was between 50 and 100 m thick and had the upper limit at about 75 m depth.

20 It also had the typical signature of low oxygen and high nutrient concentrations from decay of organic matter. Water with high silicate and undersaturated in aragonite was observed at the tip of the Morris Jesup Plateau in 1991 (Figure 5) where the subsurface waters from the Canadian Basin follows the continental margin towards the Fram Strait (Rudels et al., 1994).

Water of similar signature, but less pronounced, was also seen in the north western Fram Strait in May 2002 (Figure 6). A distinct maximum in silicate was present at the Greenland continental margin and centred around a salinity of 33. It was

25 associated with a minimum in pH and thus also in $\Omega^{aragonite}$, but with a less pronounced oxygen minimum (AOU maximum)

5 Discussion

The two major factors that impact calcium carbonate solubility in the surface ocean are salinity and pH. In the open ocean the latter is mainly determined by CO_2, either controlled by exchange with the atmosphere or through primary production / decay of organic matter. As is directly evident from Fig. 2, decay of organic matter is an important process in shelf bottom

30 waters of the Siberian shelf seas. Low $\Omega^{aragonite}$ and $\Omega^{calcite}$ values are associated with high pCO_2 (low pH) and high nutrient concentrations as well as low oxygen (high AOU). The corrosive water extending out into the deep basin is strongly

correlated with high pCO_2 (Figure 3) and high nutrients, further illustrating that decay of organic matter also here is the cause of this signature.

However, mixing with low salinity water also has an impact, especially on the shelf where the influence from river discharge is stronger and melting sea ice occurs. As illustrated in Figure 7a aragonite under-saturation is found in most surface waters

5 of salinity < 28, waters that are found north of the New Siberian Islands (Figure 2). In this region the nitrate concentration is very low, illustrating that phytoplankton blooms are well advanced and that nitrate is the limiting nutrient as the phosphate concentration is high (Figure 2). Despite recent primary production, CO_2 is slightly supersaturated and oxygen is close to equilibrium, i.e. AOU is around zero. Hence some process must compensate for the CO_2 that is consumed by primary production, and this is likely decay of terrestrial organic carbon (Anderson et al., 2009).

10 The very high silicate concentrations indicate that mainly river runoff and not sea-ice melt is the source of freshwater to low salinity waters. Consequently, this region is most likely heavily impacted by the plume of the big Siberian Rivers, here dominated by the Lena River. As CO_2 is supersaturated strongly indicates that the river runoff do not only lower the calcium and carbonate concentrations by dilution, but also decreases pH by either addition of high pCO_2 river water or by decay of organic carbon added by the river runoff. Considering a freshwater residence time on the Laptev shelf of several years

15 (Schlosser et al., 1994) the latter is the most plausible explanation.

The dilution is not a dominating process of low $\Omega^{aragonite}$ throughout the water column in the study region as seen in a DIC – TA plot (Figure 7b). The degree of saturation varies more with shifts in DIC by air-sea exchange (arrow 1) and primary production / organic matter decay (arrow 3) than dilution (arrow 2), where the latter has an effect on both TA and DIC. No clear trend can be seen when $\Omega^{aragonite}$ is plotted as a function of salinity (Figure 7c) and the data certainly do not follow the

20 dilution line, even if there are less water supersaturated at the lower salinities. Rather, the low $\Omega^{aragonite}$ is associated with high PO_4 implying organic matter decay as the main cause. This conclusion is strengthened by the correlation between $\Omega^{aragonite}$ and AOU (Figure 7d). A line is drawn that represents a typical surface water (S = 33, T= -1 $^{\circ}$C, PO_4 = 1 µmol/L, NO_3 = 16 µmol/L, AOU = 0, DIC = 2046 µmol/kg, TA = 2169 µmol/kg) that is impacted by primary production and decay of organic matter having the classical RKR ratio of the elements C:N:P:O_2 = 106:1:16:-138. Most of the data, in general,

25 follow the shape of this line even if the spread is substantial. It should be noted that all data collected during the expedition is included, i.e. including water originating from both the Atlantic and the Pacific Oceans with large variability in time since contact with the atmosphere. One example is the blue data that deviates from the line in the upper left of the graph, which likely is a result of photosynthesis in the surface water where outgassing of oxygen to the atmosphere is faster than the uptake of CO_2. These are surface waters of salinities around 32 (Figure 7a & c).

30 The low $\Omega^{aragonite}$ water observed along the continental margin (Figure 3) likely flows to the east and spreads out into the deep basin. In 2005 it was seen in the Canada Basin (Figure 4) and likely confined to the Beaufort Gyre and hence its extension depends on the atmospheric pressure field (e.g. Proshutinsky et al., 2009; Carmack et al., 2016). Decadal variability in the fresh water content of the Beaufort Gyre experienced a significant change in the 1990s, forced by a change

of the atmospheric circulation regime. For instance, in 1979 silicate concentrations as high as 40 µmol/L were observed over the Lomonosov ridge close to the North Pole during the LOREX ice camp (Moore et al., 1983), but in 1991 the silicate maximum was completely absent even in the Makarov Basin close to the North Pole (Anderson et al., 1994). One consequence of this variable extent of the Beaufort Gyre is that the export of the high nutrient, low $\Omega^{aragonite}$ water out into

5 the North Atlantic Ocean is fluctuating with time.

Jones et al. (2003) traced Pacific-originating water by its nitrate to phosphate relationship into the North Atlantic Ocean and found significant fractions in the Fram Strait, the Denmark Strait, and the Labrador Sea, but variable between different years. For many of the cruises discussed by Jones et al. (2003) there were no carbonate system data measured and hence $\Omega^{aragonite}$ could not be computed. However, it is evident that the aragonite undersaturated water is well confined to the high nutrient of

10 the high "Pacific water N-P relation" signature (Figure 8). Hence, this undersaturated water is also likely exported well into the North Atlantic Ocean.

The 2002 observations show a minimum of less than 1.4 in aragonite saturation, but not undersaturated, in the north western Fram Strait (Figure 6). This minimum is centred around a salinity of 33, but the computed fraction of Pacific Water was about 2% with the major fraction of freshwater being river runoff (Jones et al., 2008b). Hence, the signature of calcium

15 carbonate undersaturation was diluted from the source to the observation of this investigation.

However, when one compares the conditions of the waters flowing into the Arctic Ocean in the West Spitsbergen Current and the one flowing out in the East Greenland Current there are distinct differences (Figure 9). The silicate concentration is at least 2 µmol/l higher in the top 200 m while the $\Omega^{aragonite}$ values are in the order 0.2 lower in the top 100 m. This is most likely a result of addition of freshwater by both river runoff and sea ice melt, but even more important is the decay of organic

20 matter. The effect by freshening can decrease $\Omega^{aragonite}$ by no more than 0.05 under the conditions observed, pointing to the importance of organic matter decay during the circulation of these waters in the Arctic Ocean.

6 Conclusions

Corrosive surface water is exported to the central Arctic Ocean by the plume of the big Siberian Rivers, dominated by the Lena River in the Laptev – East Siberian Seas region. This signature is maintained in the shelf by microbial degradation of

25 organic matter that to a large degree is of terrestrial origin. Mixing and uptake of CO_2 from the atmosphere prevent the calcium carbonate undersaturated water to spread out far from the continental margin.

Highly calcium carbonate corrosive waters are produced along the bottoms of the East Siberian Seas through degradation of organic matter. This water is exported into the deep Makarov and Canada Basins at a depth range of about 50-150 metres. The signature of this subsurface water is maintained within the Beaufort Gyre and is exported out to the North Atlantic

30 through eastern Fram Strait, and likely also through the Canadian Arctic Archipelago.

The salinity range of this water is 32-34 and there is a potential for this water to be mixed up to layers inhabited by aragonite forming organisms such as pteropods. Such mixing can be either a result of wind or through sea ice formation when the surface layer gets homogenized by brine release, or when it enters the East Greenland Current.

Acknowledgments

5 This research was supported by the Swedish Knut and Alice Wallenberg Foundation (KAW); the Swedish Research Council, VR (L.G.A. 621-2013-5105); the Swedish Research Council Formas (A.U. #2014-1165). We thank the supporting crew and Captain of I/B Oden as well as the support of the Swedish Polar Secretariat.

References

Anderson, L.G., Björk, G., Holby, O., Kattner, G., Koltermann, P.K., Jones, E.P., Liljeblad, B., Lindegren, R., Rudels, B.,
10 and Swift, J.: Water Masses and Circulation in the Eurasian Basin: Results from the Oden 91 North Pole Expedition, J. Geophys. Res., 99, 3273-3283, 1994.

Anderson L.G., Jutterström, S., Hjalmarsson, S., Wåhlström I., and Semiletov, I.P.: Out-gassing of CO_2 from Siberian Shelf Seas by terrestrial organic matter decomposition, Geophys. Res. Lett., 36, L20601, doi:10.1029/2009GL040046, 2009.

Anderson L.G., Tanhua, T., Björk, G., Hjalmarsson, S., Jones, E.P., Jutterström, S., Rudels, B., Swift, J. H., and Wåhlström,
15 I.: Arctic Ocean shelf – basin interaction, an active continental shelf CO_2 pump and its impact on the degree of calcium carbonate dissolution, Deep Sea Res., I 57, 869–879 doi:10.1016/j.dsr.2010.03.012, 2010.

Azetsu-Scott, K., Clarke, A., Falkner, K., Hamilton, J., Jones, E.P., Lee, C., Petrie, B., Prinsenberg, S., Starr, M., and Yeats, P.: Calcium carbonate saturation states in the waters of the Canadian Arctic Archipelago and the Labrador Sea, J. Geophys. Res., 115: C11021, 2010.

20 Carmack, E., and Wassmann, P.: Food webs and physical–biological coupling on pan-Arctic shelves: Unifying concepts and comprehensive perspectives, Prog. Ocean., 71(2-4), 446-477, doi:10.1016/j.pocean.2006.10.004, 2006.

Carmack, E. C., Yamamoto-Kawai, M., Haine, T.W.N., Bacon, S., Bluhm, B.A., Lique, C., Melling, H., Polyakov, I.V., Straneo, F., Timmermans, M.-L., and Williams, W.J.: Freshwater and its role in the Arctic Marine System: Sources, disposition, storage, export, and physical and biogeochemical consequences in the Arctic and global oceans, J. Geophys.
25 Res. Biogeosci., 121, 675–717, doi:10.1002/2015JG003140, 2016.

Clayton, T.D., and Byrne, R.H.: Spectrophotometric seawater pH measurements: total hydrogen ion concentration scale calibration of m-cresol purple at-sea results. Deep-Sea Res., I, 40(10), 2115-2129, 1993.

Dieckmann, G.S., Nehrke, G., Papadimitriou, S., Göttlicher, J., Steininger, R., Kennedy, H., Wolf-Gladow, D., and Thomas, D.N.: Calcium carbonate as ikaite crystals in Antarctic sea ice, Geophys. Res. Lett., 35, L08501,
30 doi:10.1029/2008GL033 540, 2008.

Doney, S.C., Fabry, V.J., Feely, R.A., Kleypas, J.A.: Ocean acidification: the other CO_2 problem, Ann. Rev. Mar. Sci., 1(1), 169-192, doi:10.1146/annurev.marine.010908.163834, 2009.

Findlay H.S., Wood H.L., Kendall M.A., Spicer J.I., Twitchett R.J. and Widdicombe S.: Comparing the impact of high CO2 on calcium carbonate structures in different marine organisms, Marine Biol. Res., 7, 565-575, 2011.

5 Gattuso, J.-P., Magnan, A., Billé, R., Cheung, W.W.L., Howes, E.L., Joos, F., Allemand, D., Bopp, L., Cooley, S.R., Eakin, C.M., Hoegh-Guldberg, O., Kelly, R.P., Pörtner, H.-O., Rogers, A.D., Baxter, J.M., Laffoley, D., Osborn, D., Rankovic, A., Rochette, J., Sumaila, U.R., Treye, S., Turley C.: Contrasting futures for ocean and society from different anthropogenic CO2 emissions scenarios, Science, 349, 6243, doi:10.1126/science.aac4722, 2015.

Haraldsson, C., Anderson, L.G., Hassellöv, M., Hulth, S.: Rapid, high-precision potentiometric titration of alkalinity in
10 ocean and sediment pore waters, Deep-Sea Res., 44, 2031-2044, 1997.

Johnson, K.M., Sieburth, J.M., Williams, P.J., and Brandström, L.: Coulometric total carbon dioxide analysis for marine studies: automation and calibration, Mar. Chem., 21, 117-133, 1987.

Jones, E.P., Swift, J.H., Anderson, L.G., Lipizer, M., Civitarese, G., Falkner, K., Kattner G., and McLaughlin, F.: Tracing Pacific Water in the North Atlantic Ocean, J. Geophys. Res., 108(C4), 3114, doi:10.1029/2001JC001141, 2003.

15 Jones, E.P., Anderson, L.G., Jutterström, S., Mintrop, L., and Swift, J.H.: Pacific freshwater, river water and sea ice meltwater across Arctic Ocean basins: Results from the 2005 Beringia Expedition, J. Geophys. Res., 113, C08012, doi:10.1029/2007JC004124, 2008a.

Jones E.P., Anderson, L.G., Jutterström, S., and Swift, J.H.: Sources and Distribution of Fresh water in the East Greenland Current, Prog. Ocean., 78, 37-44, doi: 10.1016/j.pocean.2007.06.003, 2008b.

20 Jutterström, S., Jeansson, E., Anderson, L.G., Bellerby, R., Jones, E.P., Smethie Jr., W.M., and Swift, J.H.: Evaluation of anthropogenic carbon in the Nordic Seas using observed relationships of N, P and C versus CFCs, Prog. Ocean., 78, 78-84, doi: 10.1016/j.pocean.2007.06.001, 2008.

Jutterström, S., and Anderson, L.G.: Uptake of CO_2 by the Arctic Ocean in a changing climate, Mar. Chem., 122, 96-104, doi:10.1016/j.marchem.2010.07.002, 2010.

25 Legge, O.J., Bakker, D.C.E., Johnson, M.T., Meredith, M.P., Venables, H.J., Brown, P.J., and Lee, G.A.: The seasonal cycle of ocean-atmosphere CO2 flux in Ryder Bay, west Antarctic Peninsula, Geophys. Res. Lett., 42, 2934–2942, doi:10.1002/2015GL063796, 2015.

Liu, X., Patsavas, M.C., and Byrne, R.H.: Purification and Characterization of meta-Cresol Purple for Spectrophotometric Seawater pH Measurements. Environ. Sci. Tech., 45(11), 4862-4868, doi:10.1021/es200665d, 2011.

30 Lueker, T.J., Dickson, A.G., Keeling, C.D.: Ocean pCO2 calculated from dissolved inorganic carbon, alkalinity, and equations for K1 and K2: validation based on laboratory measurements of CO2 in gas and seawater at equilibrium. Mar. Chem., 70, 105-119, 2000.

Moore, R.M., Lowings, M.G., Tan, F.C.: Geochemical profiles in the Central Arctic Ocean: Their relation to freezing and shallow circulation. J. Geophys. Res., 88, 2667-2674, 1983.

Orr, J.C., Fabry, V.J., Aumont, O., Bopp, L., Doney, S.C., Feely, R.A., Gnanadesikan, A., Gruber, N., Ishida, A., Joos, F., Key, R.M., Lindsay, K., Maier-Reimer, E., Matear, R., Monfray, P., Mouchet, A., Najjar, R.G., Plattner, G.-K., Rodgers, K.B., Sabine, C.L., Sarmiento, J.L., Schlitzer, R., Slater, R.D., Totterdell, I.J., Weirig, M.-F., Yamanaka, Y., and Yoo, A.: Anthropogenic ocean acidification over the twenty-first century and its impact on calcifying organisms. Nature, 437, doi:10.1038/nature04095, 2005.

Proshutinsky, A., Krishfield, R., Timmermans, M.-L., Toole, J., Carmack, E., McLaughlin, F., Williams, W.J., Zimmermann, S., Itoh, M., and Shimada, K.: Beaufort Gyre freshwater reservoir: State and variability from observations, J. Geophys. Res., 114, C00A10, doi:10.1029/2008JC005104, 2009.

Rudels, B., Jones, E.P., Anderson L.G., and Kattner, G.: On the intermediate depth waters of the Arctic Ocean, in The Polar Oceans and Their Role in Shaping the Global Environment, edited by O.M. Johannessen R.D. Muench and J.E. Overland, pp. 33-46, American Geophysical Union, Washington, D.C., 1994.

Schlosser, P., Bauch, D., Fairbanks, R., and Bonisch, G.: Arctic river runoff: Mean residence time on the shelves and in the halocline, Deep Sea Res., Part I, 41, 1053–1068, doi:10.1016/0967-0637(94)90018-3, 1994.

Semiletov, I., Pipko, I., Gustafsson, Ö., Anderson, L.G., Sergienko, V., Pugach, S., Dudarev, O., Charkin, A., Gukov, A., Bröder, L., and Shakhova, N: Extreme acidification in the East Siberian Arctic Shelf driven by a permafrost-released carbon translocation and seawater freshening. Nature Geoscience, 18 April, doi:10.1038/NEGO2695, 2016.

van Heuven, S., Pierrot, D., Rae, J.W.B., Lewis, E., and Wallace, D.W.R.: MATLAB Program Developed for CO2 System Calculations. ORNL/CDIAC-105b. Carbon Dioxide Information Analysis Center, Oak Ridge National Laboratory, U.S. Department of Energy, Oak Ridge, Tennessee. doi:10.3334/CDIAC/otg.CO2SYS_MATLAB_v1.1, 2011.

Yamamoto-Kawai, M., Mclaughlin, F.A., Carmack, E.C., Nishino, S., Shimada, K.: Aragonite undersaturation in the Arctic Ocean: effects of ocean acidification and sea ice melt. Science, 326, 1098–1100, doi:10.1126/ science.1174190, 2009
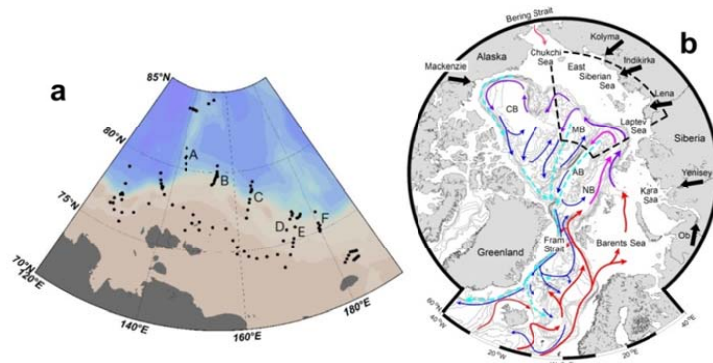
Figure 1. Map illustrating the station locations, with (a) sections noted and (b) general water mass circulation in the deep Arctic Ocean and its connection to surrounding oceans. The location of map in (a) is shown by the dotted insert in map (b).
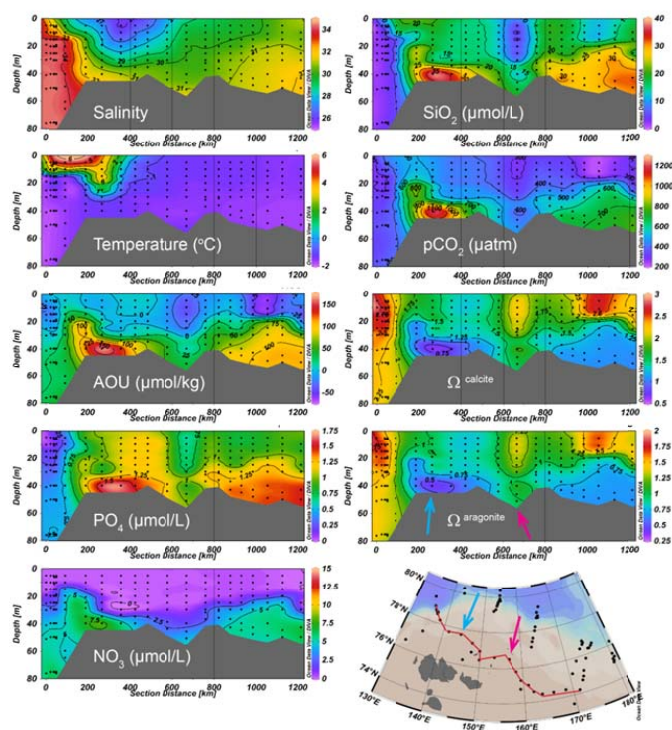
5   **Figure 2.** Sections along the outer East Siberian continental shelf as shown by the red line of the map. The location of the minimum in saturation state of calcium carbonate is noted by the blue arrow and the local maximum by the purple arrow.
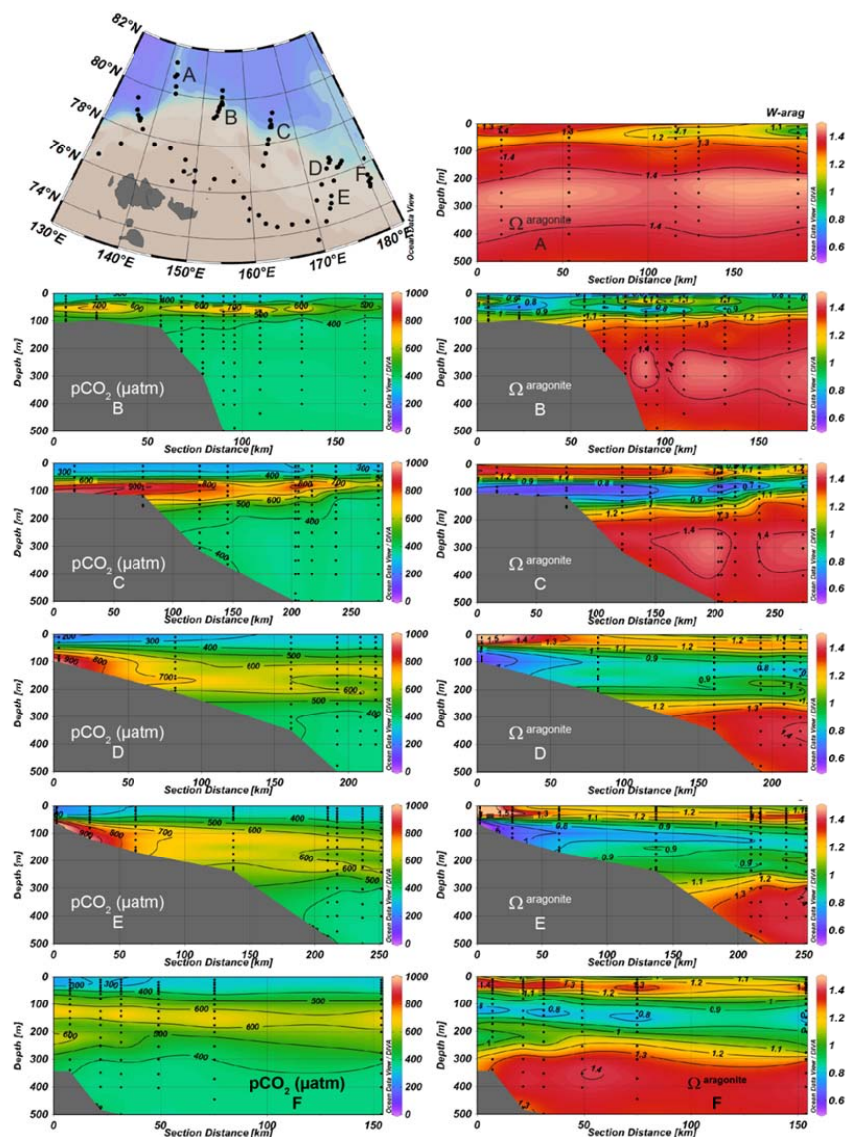
Figure 3. Sections A to F across the East Siberian shelf break, partial pressure of carbon dioxide (pCO₂) to the left and saturation state of aragonite (Ω^{aragonite}) to the right. On all sections the colour scale is from 0 to 1000 µatm for pCO₂ and 0.5 to 1.5 for Ω^{aragonite}. Note the variable horizontal extent of the different sections. The locations of the sections are noted on the inserted map.
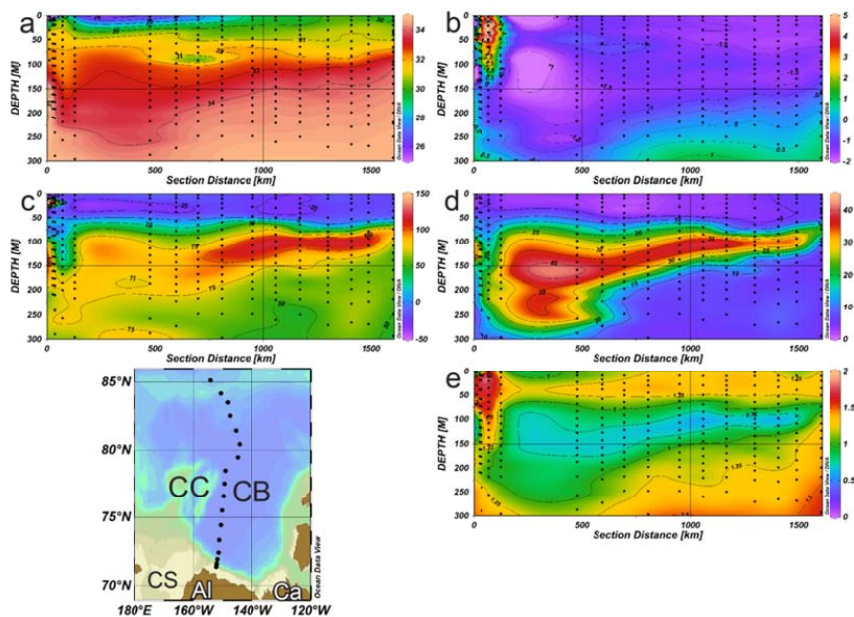
Figure 4. Sections of (a) salinity, (b) temperature, (c) AOU, (d) silicate, and € $\Omega^{aragonite}$ in the top 300 m across the Canada Basin as observed during the Beringia 2005 expedition. Station positions are noted on the map, with the abbreviations being; CB = Canadian Basin, CC = Chukchi Cape, CS = Chukchi Sea, Al = Alaska, and Ca = Canada.
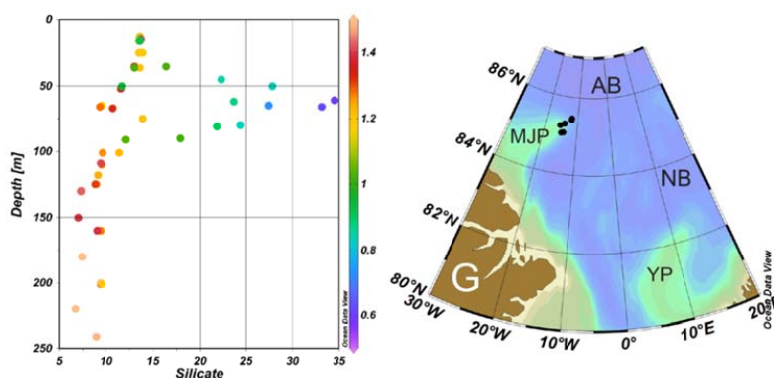
Figure 5. Silicate profiles of six stations over the Morris Jesup Plateau (MJP), colour coded by $\Omega^{aragonite}$, as observed during the Oden 91 cruise. Station positions are noted on the map, with the abbreviations being; AB = Amundsen Basin, NB = Nansen Basin, YP = Yermak Plateau, and G = Greenland.
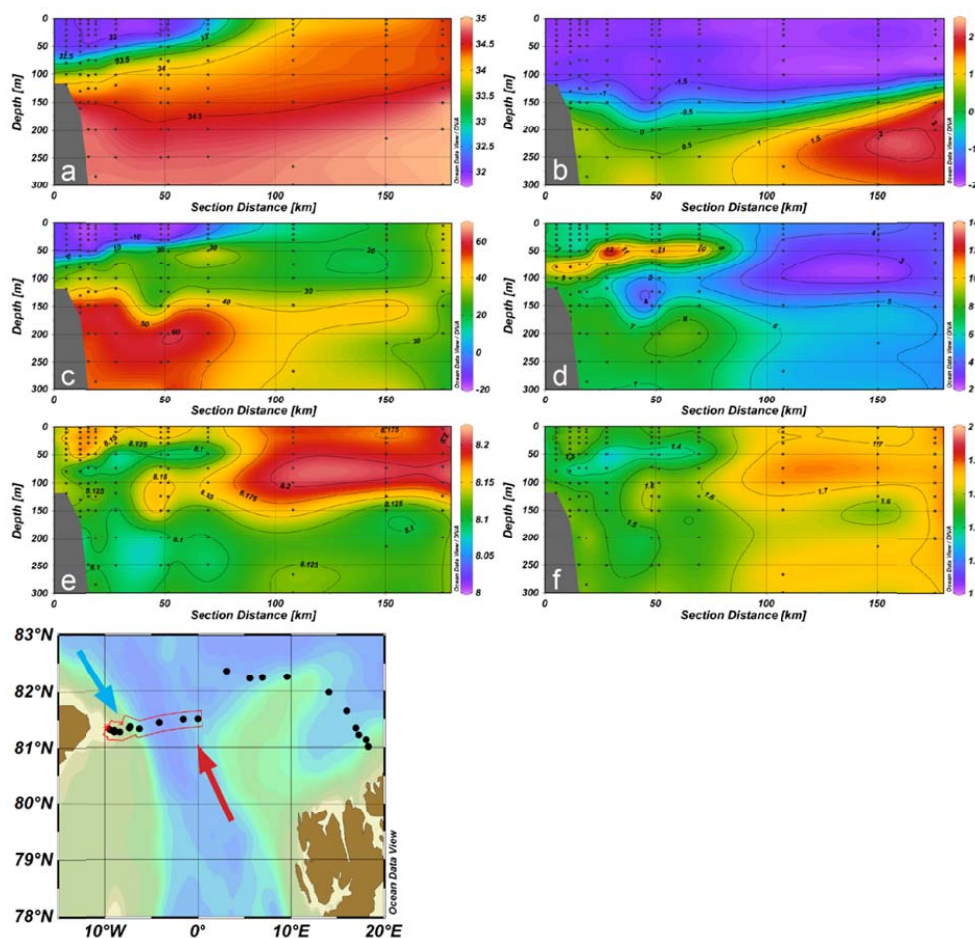
Figure 6. Sections of (a) salinity, (b) temperature, (c) AOU, (d) SiO₂, (e) pH$^{tot}_{in\ situ}$, and (f) Ω^{aragonite}, across the northen Fram Strait at about 81.5 °N from the Yermak Plateau to Greenland as noted on the map, collected in May 2002. The arrows illustrate the north flowing warm Atlantic and the southflowing cold Arctic surface waters.
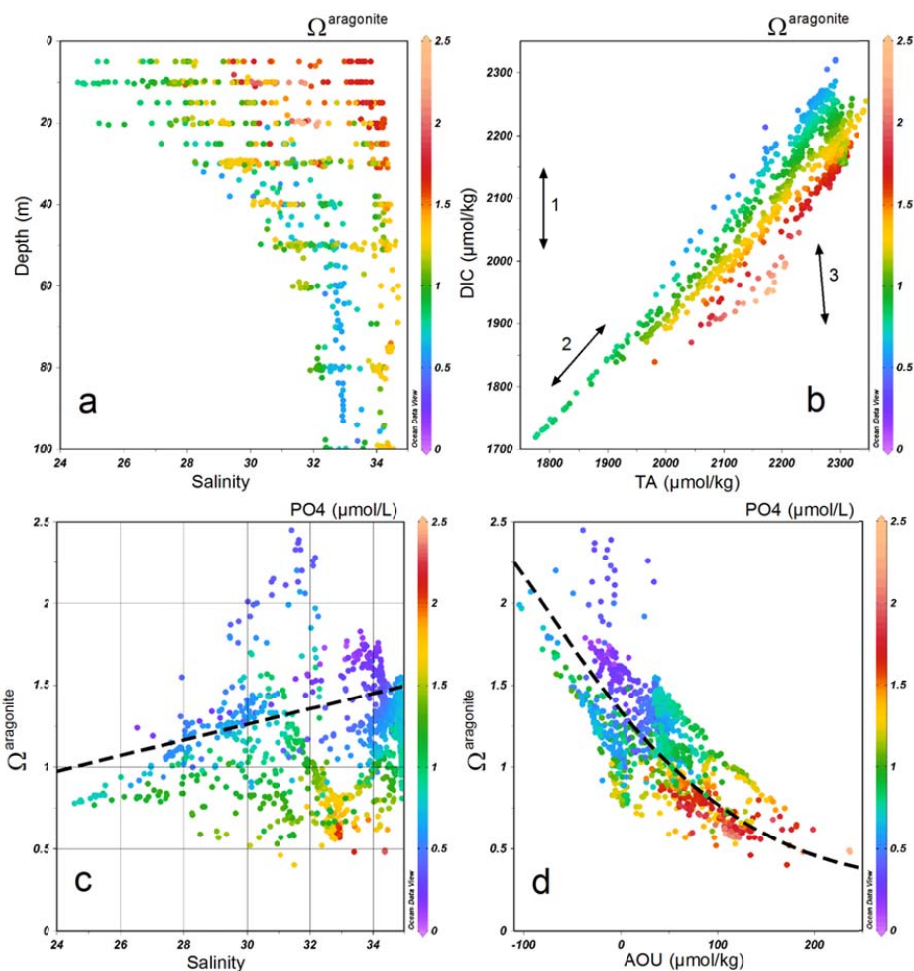
Figure 7. Plot of a) salinity versus depth b) DIC versus TA, both colour coded by $\Omega^{aragonite}$, c) $\Omega^{aragonite}$ versus salinity, colour coded by Apparent Oxygen Saturation (AOU) and d) $\Omega^{aragonite}$ versus AOU, colour coded by PO_4. In b) arrows are drawn to illustrate the impact by air-sea CO_2 gas exchange (1), dilution of water with zero DIC and TA (2) and primary production (down) and decay of organic matter (3). In c) a line is drawn that represents the theoretical impact of dilution of Atlantic Layer Water (S = 34.85, T= -1 °C, DIC = 2170 µmol/kg, TA = 2300 µmol/kg) with water of zero S, DIC and TA, and in d) a line is drawn that represents a typical surface water (S = 33, T= -1 °C, PO_4 = 1 µmol/L, NO_3 = 16 µmol/L, AOU = 0, DIC = 2046 µmol/kg, TA = 2169 µmol/kg) that is impacted by primary production and decay of organic matter of the classical RKR ratio of C:N:P:O_2 = 106:1:16:-138.
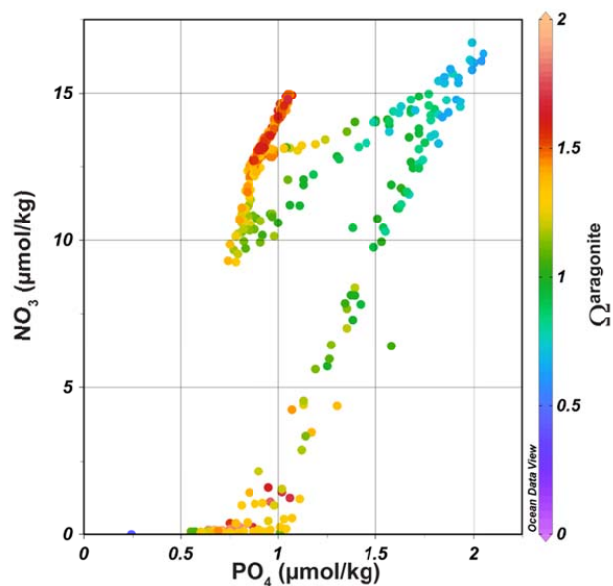
Figure 8. Nitrate versus phosphate as observed in the Canada Basin during the Beringia 2005 expedition (station locations same as in Fig. 4), colour coded by $\Omega^{aragonite}$.
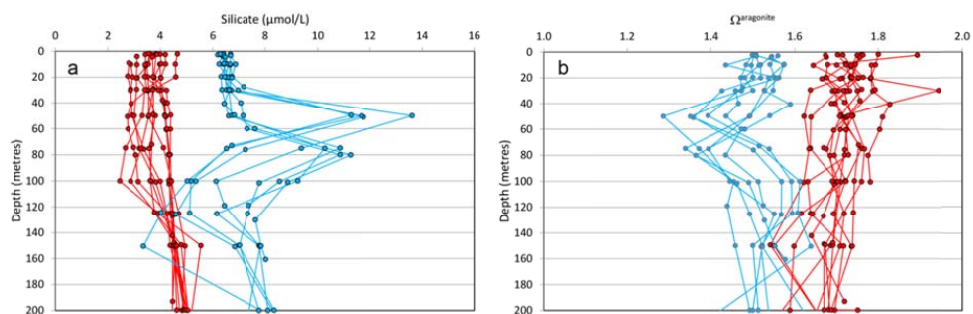
5   **Figure 9. Depth profiles of silicate (a) and $\Omega^{aragonite}$ (b) in the Fram Strait around 82° N in 2002. The 2002 are all computed from pH and TA and covers the whole strait. In the latter one can notice the clear division of the north flowing Atlantic water (red with a surface salinity around 34.5) and the south flowing Arctic Waters (blue with a surface salinity around 32). Both in and outflowing water has a surface temperature below -1 °C making the salinity and temperature effect on $\Omega^{aragonite}$ in the order of max 0.05.**